

# Bidimensional Analysis of the Phase Behavior of a Well-Defined Surfactant (C<sub>10</sub>E<sub>4</sub>)/Oil (*n*-Octane)/Water–Temperature System

Aldo Pizzino,<sup>\*,†,‡</sup> Valérie Molinier,<sup>‡</sup> Marianne Catté,<sup>‡</sup> Jean-Louis Salager,<sup>†</sup> and Jean-Marie Aubry<sup>‡</sup>

Laboratorio FIRP, Ingeniería Química, Universidad de Los Andes, Mérida 5001, Venezuela, and LCOM, Equipe “Oxydation et Physico-Chimie de la Formulation”, UMR CNRS 8009, ENSCL, Université de Lille 1, BP 90108, 59652 Villeneuve d’Ascq Cedex France

Received: July 29, 2009; Revised Manuscript Received: October 15, 2009

The equilibrium phase behavior of the well-defined system tetraethyleneglycol decyl ether (C<sub>10</sub>E<sub>4</sub>)/*n*-octane/water (SOW) at variable temperature (*T*) was revisited by careful analysis of the three bidimensional cuts, namely, the  $\gamma$  (at constant water–oil ratio),  $\chi$  (at constant surfactant concentration), and  $\Delta$  (at constant temperature) plots. A straightforward methodology is reported to determine the frontiers of the triphasic (Winsor III) domain on any cut of the SOW–*T* phase prism. It comes from the systematic analysis of another cut, here  $\gamma$  at different water–oil ratios and  $\chi$  at different surfactant concentrations from the knowledge of  $\Delta$  cuts at different temperatures. The method has been validated through comparison with experimental results. It enables one to show, for the first time, the evolution of a SOW system three-phase body contours with (i) water–oil ratio, (ii) surfactant concentration, and (iii) temperature. It exhibits a strong impact of the surfactant affinity for the pure oil and water phases on the shape of the phase diagrams. The systematic study of the effect of the surfactant concentration on the aspect of the  $\chi$  plot sheds light on an unusual shape found at low surfactant concentration.

## 1. Introduction

The phase behavior is the state of thermodynamic equilibrium of a given system. For a ternary surfactant/oil/water (SOW) system, the study of phase equilibria is of the utmost importance in applications such as solubilization of organic compounds, surface cleaning, and emulsification of oils, etc., and depends on the action of the surfactant on the water–oil incompatibility.<sup>1</sup> Moreover nonequilibrium properties such as the morphology and stability of emulsions have been directly related to the phase behavior.<sup>2–5</sup>

The phase behavior depends on formulation and composition variables. On the one hand, the formulation variables are the one that can change the relative affinity of the surfactant for the aqueous and oil phases. Among them, the internal ones are those factors related to the components of the system such as surfactant structure, the nature of the oily phase, salinity, pH, alcohol type, and concentration. Pressure and temperature (*T*) are the so-called external formulation variables. On the other hand, the composition variables are the ones that allow locating the system in a ternary diagram, e.g., the surfactant concentration and the water–oil ratio.<sup>6</sup>

According to the phase rule, a SOW ternary system at constant pressure and temperature may form a maximum of three phases at equilibrium. This three-phase occurrence is due to the superposition of the three binary solubility gaps<sup>7,8</sup> and is generally referred to as a Winsor III case. A Winsor III system is composed of an oil and water bicontinuous surfactant-rich microemulsion in equilibrium with oil and aqueous excess phases. A two-phase system is of the Winsor I (respectively II) type, when a surfactant-rich aqueous (respectively oil) phase is at equilibrium with an oil (respectively aqueous) excess phase.<sup>9</sup>

For a system based on a nonionic polyethoxylated surfactant, temperature can change the affinity of the surfactant for the aqueous and oil phases, thus allowing the change from a Winsor-type to the other. At high surfactant concentration or at very high or very low water–oil ratio, a monophasic system is found. This phase is said to be of the Winsor IV type and can exhibit complex mesophasic structures.

To represent the phase behavior of a SOW system as a function of two composition variables (water–oil ratio and surfactant concentration) and a formulation variable (often temperature for a polyethoxylated surfactant-based system), a three-dimensional representation is required. As a consequence, the phase behavior of a SOW system based on a polyethoxylated surfactant is a triangular prism with the ternary SOW as the basis and temperature as the vertical axis. Classically, 2-D representations are preferred for the sake of simplicity, and, depending on the property to be enlightened, one of the three cuts of this prism is used: the  $\Delta$  (constant temperature),  $\gamma$  (constant water–oil ratio),  $\chi$  (constant surfactant concentration) representations (cf. Figure 1).<sup>5,10</sup>

The  $\Delta$  and  $\gamma$  representations (Figures 1 left, 1 center) are useful to know the minimum amount of surfactant required to attain a monophasic system. The  $\Delta$  cut exhibits the effects of both the surfactant concentration and water–oil ratio on the phase behavior but does not show the influence of the formulation variable (temperature). The  $\gamma$  cut presents the combined effects of the formulation variable (temperature) and the surfactant concentration and gives access to an important parameter for applications that is the efficiency of the surfactant.<sup>11</sup> The  $\chi$  representation is the most appropriate one to locate the boundary between the O/W and W/O morphologies of emulsions, i.e., the so-called “standard inversion line”, since it simultaneously shows the effects of both formulation (temperature) and water–oil ratio.<sup>4,5,12</sup> The position of the triphasic

<sup>†</sup> Universidad de Los Andes.

<sup>‡</sup> Université de Lille 1.

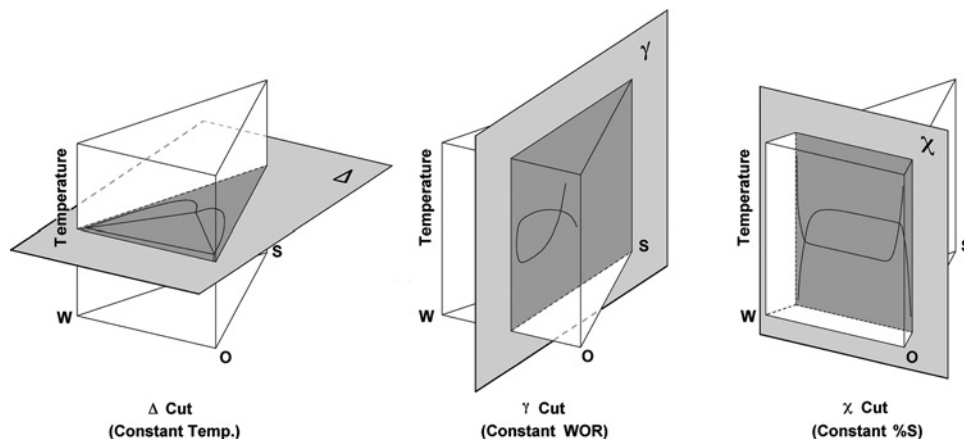


**Figure 1.** Bidimensional cuts of a surfactant/oil/water–temperature prism: (left) at constant temperature ( $\Delta$  cut), (center) constant water–oil ratio ( $\gamma$  cut), or (right) constant surfactant concentration ( $\chi$  cut).

(Winsor III) domain is particularly crucial to locate, since, due to the ultralow interfacial tensions,<sup>3,13,14</sup> it is where the emulsification is the easiest, but also where the emulsions are the less stable, and where the phase inversion can take place.<sup>4</sup>

The phase behavior of simple ternary systems consisting of water, oil, and a nonionic surfactant of the polyethoxylated alcohol or phenol type has been the subject of numerous detailed studies during the past decades.<sup>15–17</sup>  $\chi$  representations were first studied for systems based on mixtures of alkylphenoethoxylates<sup>1,18</sup> and from the 1980s, the data started to be implemented with  $\gamma$  and  $\Delta$  representations for systems based on polyethoxylated alcohols ( $C_iE_j$ ).<sup>7,8,18–22</sup> This class of amphiphile is particularly convenient for systematic analysis of phase behavior since by varying the alkyl chain length ( $i$ ) and the number of ethylene oxide groups per molecule ( $j$ ), the hydrophilic–lipophilic balance may be continuously tuned and the amphiphilicity can be changed from weak ( $i \leq 8, j \leq 3$ ) to strong.<sup>23–25</sup> Kahlweit and co-workers have collected numerous data on these systems and have presented a comprehensive three-dimensional interpretation of the phase behavior.<sup>11,20,26–31</sup> Systematic studies have been usually performed on short-chain  $C_iE_j$ , such as for instance  $C_4E_1$  and  $C_4E_2$ <sup>32–34</sup> because the systems based on these weak amphiphiles exhibit the same features as the ones containing a surfactant,<sup>26</sup> though they are easier to handle particularly because they do not form mesophases at high concentrations and are more easily quantified.

In the present work, the phase behavior of a model SOW based on an oligomerically pure surfactant ( $C_{10}E_4$ ) and a pure oil ( $n$ -octane) has been studied. A  $\gamma$  cut at water–oil ratio = 1 and a  $\chi$  representation at 15% (w/w) surfactant have already been published for this system,<sup>29,35</sup> whereas the  $\Delta$  representation has been presented with hexadecane as the oil phase.<sup>36,37</sup> However, no systematic study has been reported to correlate the phase equilibrium data with the emulsion properties. This is the purpose of the present work that will be presented in this and forthcoming companion papers. The aqueous phase contains a low amount of electrolyte ( $10^{-2}$  M NaCl) in order to easily detect the emulsion external phase by conductimetry. In this work, a methodology is presented to determine the boundary of the three-phase body on any cut of the phase prism, from the systematic study of one of the two others. Particularly, this allows one to follow the evolution of the three-phase body on the  $\gamma$  cut with the water–oil ratio and on the  $\chi$  cut with the surfactant concentration.

## 2. Experimental Section

**2.1. Chemicals and General Methods.** The pure tetraethyleneglycol monodecyl ether ( $C_{10}E_4$ ) was synthesized according to a method described elsewhere.<sup>38–40</sup> The purity was assessed by NMR and GC analyses (>99%) and by determining the cloud point temperature.<sup>41</sup> The compound was distilled under reduced pressure (at least three times consecutively) until obtaining a cloud point temperature in agreement with the published data (20.0 °C/2.6% (w/w); lit.,<sup>39</sup> 20.56 °C/2.6% (w/w)). Deionized water (1.34  $\mu$ S/cm at 25 °C), sodium chloride (Aldrich, >99%), and  $n$ -octane (Aldrich, >99%) were used for the preparation of the aqueous and oil phases. For GC analyses, samples were prepared in absolute ethanol (Merck) and  $n$ -decane (Aldrich, >99%) was used as an internal standard.

Gas chromatography (GC) analyses were performed on an Agilent 6890N apparatus, equipped with a HP-1 cross-linked methyl silicone gum column (60 m  $\times$  0.32 mm  $\times$  0.25  $\mu$ m), with  $N_2$  as gas vector and with a flame ionization detector (FID).

**2.2. Construction of the Phase Diagrams.** All samples were prepared by weight, and the concentrations given below, unless otherwise stated, are in weight percent (wt %). The aqueous phase was a  $10^{-2}$  M NaCl solution in water. Pure  $n$ -octane was used for the oil phase. The glass vials for the determination of  $\Delta$  diagrams and the sealed glass tubes (internal diameter, 5 mm; total volume, 1.2 mL) for the determination of  $\gamma$  and  $\chi$  diagrams were prepared by successively adding the  $10^{-2}$  M NaCl solution,  $n$ -octane, and  $C_{10}E_4$ . The samples were gently shaken to facilitate the contact between the phases and placed in a thermostatted bath at constant temperature ( $\pm 0.1$  °C) until the equilibrium was reached, i.e., until complete phase separation, which usually took from several hours to a few weeks.

**2.2.1. Delta ( $\Delta$ ) Diagram.** The triphasic domain on the  $\Delta$  diagram was determined by GC quantification at eight temperature values: 22.2, 23.0, 24.0, 25.0, 25.6, 27.0, 28.0, and 28.6 °C. Experiments were performed in duplicate.

The 5 g samples were prepared at  $fw = 0.5$ .  $fw$  is the water weight fraction defined as follows:  $fw = W/(W + O)$ , where  $W$  (respectively  $O$ ) is the weight of the water phase (respectively oil phase). The total amount of  $C_{10}E_4$  was 3%. When the samples were completely equilibrated, known and precise amounts of the oil and middle phases were withdrawn carefully by means of a syringe. Typically, the amount of each phase sample taken out was in the range of 0.3–1 g.

The whole amount was then diluted with absolute ethanol containing  $n$ -decane as an internal standard (1 mg/mL) to the

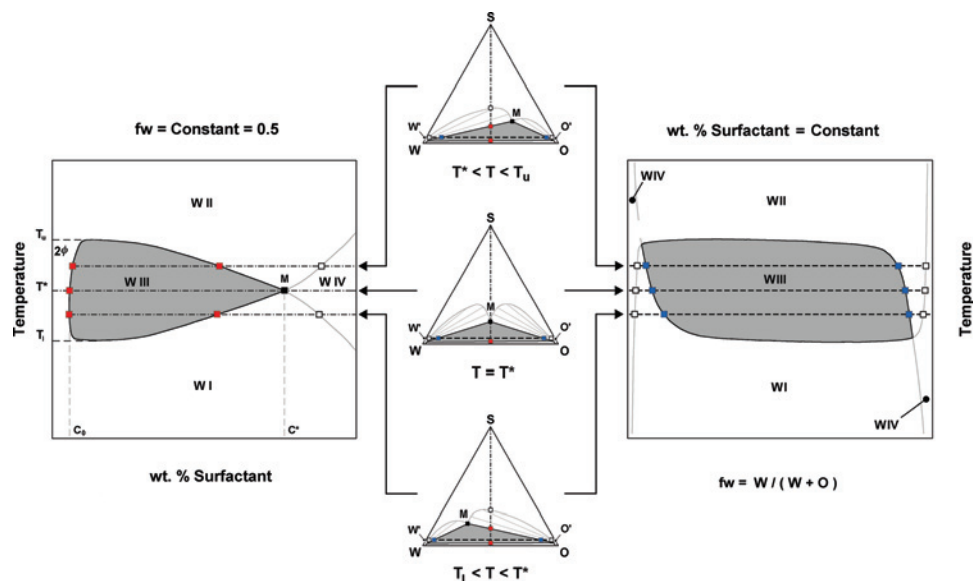


**Figure 2.** Schematic representation of the methodology used to determine the  $\gamma$  cut at constant  $fw$  (left) and  $\chi$  cut at constant surfactant concentration (right) from the  $\Delta$  cut diagrams at different temperatures (center).

proper concentration for GC quantification. A  $1 \mu\text{L}$  aliquot was injected in a splitless mode, with an inlet temperature set at  $285 \text{ }^\circ\text{C}$ . The temperature program allowed the simultaneous quantification of *n*-octane and  $\text{C}_{10}\text{E}_4$ . The oven temperature was held at  $70 \text{ }^\circ\text{C}$  for 2 min, increased to  $100 \text{ }^\circ\text{C}$  at  $5 \text{ }^\circ\text{C}/\text{min}$ , and then to  $285 \text{ }^\circ\text{C}$  at  $20 \text{ }^\circ\text{C}/\text{min}$ . It was maintained at this temperature for 10 min. This method resulted in the following retention times: 5.4 min for *n*-octane, 9.2 min for the internal standard of *n*-decane, and 22.0 min for  $\text{C}_{10}\text{E}_4$ .

Three injections were performed on the same sample to check the reproducibility of the quantification. It usually fell within 1% for *n*-octane and 2% for  $\text{C}_{10}\text{E}_4$ . A calibration curve for *n*-octane and  $\text{C}_{10}\text{E}_4$  was built beforehand on a 0.12–1.00% range for the former ( $R^2 = 0.9998$ ) and 0.05–0.15% for the latter ( $R^2 = 0.9985$ ). Both compounds were quantified in the surfactant-rich middle phase. The amount of water was obtained from the two others by difference. Only  $\text{C}_{10}\text{E}_4$  was quantified in the oil phase, in which the amount of water was assumed to be zero; hence, the amount of *n*-octane was obtained by difference to the surfactant. No quantification was performed in the aqueous phase.

**2.2.2.  $\gamma$  and  $\chi$  Diagrams.** The 1 g samples were prepared and once the equilibrium was reached at the desired temperature, the phase behavior (WI, WII, WIII, or WIV) was determined by visual observation. The position of the microemulsion phase was confirmed by use of a laser pointer (375 nm), which allows to put in evidence the presence of micelles by Tyndall effect.

### 3. Results and Discussion

#### 3.1. Methodology To Determine the Frontiers of the Three-Phase Domain in Two Cuts from the Systematic Study of the Third One.

**3.1.1. Geometrical Relations between  $\gamma$ ,  $\chi$ , and  $\Delta$  Cuts.** The characterization of the triangular phase prism  $\text{C}_{10}\text{E}_4$ /*n*-octane/water + 0.01 M NaCl–temperature was performed by simple analysis of the main characteristics of the triphasic domain of the  $\Delta$  diagram at constant temperature. A low amount of electrolyte was added to the aqueous phase to ensure the electrical conductivity needed to follow the morphology of the emulsified system that will be dealt with in forthcoming papers. It is worth noting that the presence of this low amount of NaCl

does not affect the equilibrium phase behavior of the system, as confirmed by the results presented below, which are in agreement with the published data<sup>29,34</sup> on the salt-free system.

The  $\Delta$  cuts were determined at eight temperatures by GC quantification of the surfactant  $\text{C}_{10}\text{E}_4$  (S) and oil *n*-octane (O) in the microemulsion and oil phases of the sample at equilibrium. The amount of water + NaCl (W) was obtained by difference. As a reminder here, the so-called triangular phase prism has the  $\Delta$  diagram as the basis and the temperature as vertical axis (cf. Figure 1).

Figure 2 (center) schematizes the representations of  $\Delta$  diagrams at three different temperatures:  $T_l < T < T^*$ ,  $T = T^*$ , and  $T^* < T < T_u$ , where  $T_l$  and  $T_u$  define the lower (l) and upper (u) temperature limits of the range in which the system phase behavior is of the WIII type.<sup>9,11,42</sup>  $T^*$  is the temperature for which a minimum amount  $C^*$  of surfactant is needed to reach the monophasic WIV system, for equal amounts of aqueous and oil phases.<sup>21</sup> For temperatures lower than  $T_l$  and higher than  $T_u$ , the system at equilibrium is biphasic, of the WI type (hydrophilic surfactant) and WII type (lipophilic surfactant), respectively.<sup>9,42</sup>

As may be seen on Figure 2, the  $\Delta$  diagram includes a triangular zone, displayed in gray in the figure, where the system exhibits three phases at equilibrium (WIII type): an oil phase (O'), an aqueous phase (W'), and a surfactant-rich microemulsion (M) of intermediate density, often referred to as middle-phase.

The  $\gamma$  (Figure 2, left) and  $\chi$  (Figure 2, right) diagrams can be determined by analysis of the  $\Delta$  diagrams.

At constant  $fw$ , the plane containing the  $\gamma$  diagram intersects the  $W'O'M$  triangle in the  $\Delta$  diagram at the points indicated in red on Figure 2 (center) on the dotted and dashed (---) line coming vertically from the S vertex. The intersections with  $W'O'$  and  $W'M$  or  $O'M$  correspond to the minimum and maximum surfactant concentrations, which result in a WIII system. In the  $T$  vs %S plane, these points define the WIII triphasic zone on the  $\gamma$  diagram (in gray in Figure 2, left).

In the same way, at constant surfactant concentration, the plane containing the  $\chi$  diagram intersects the triphasic zone of the  $\Delta$  diagram at the points shown in blue on the horizontal dashed (---) line (Figure 2, center). In the  $T$  vs  $fw$  plane, these

**TABLE 1: Composition of the Phases Represented by the O' and M Points in Figure 2 for the C<sub>10</sub>E<sub>4</sub>/n-Octane/10<sup>-2</sup> M NaCl System<sup>a</sup>**

point	T (°C)	O' phase		M phase	
		%S	%O	%S	%O
1	22.2	1.5	98.5	4.9	13.5
2	23.0	1.6	98.4	7.1	22.2
3	24.0	1.8	98.2	9.3	31.3
4	25.0	1.8	98.2	10.4	37.5
5	25.6	1.8	98.2	10.8	41.8
6	27.0	2.0	98.0	10.5	56.3
7	28.0	2.1	97.9	8.9	69.4
8	28.6	2.6	97.4	6.0	86.3

<sup>a</sup> %S and %O are the weight percent of C<sub>10</sub>E<sub>4</sub> and n-octane, respectively, in each phase.

points define the triphasic zone of the  $\chi$  diagram (in gray in Figure 2, right).

In addition to the W'O'M triangle, the sections obtained at constant fw and surfactant concentration also intersect the biphasic lobes on the  $\Delta$  diagram (Figure 2 center) located above W'M and O'M. These points (empty squares on Figure 2) define the frontier of the monophasic WIV zone in the  $\gamma$  and  $\chi$  diagrams (see Figure 2), which are not reported here.

To determine accurately the frontier of the three-phase domain on the  $\gamma$  and  $\chi$  diagrams, a systematical study of  $\Delta$  diagrams is required, to obtain the intersection points defined above at different temperatures.

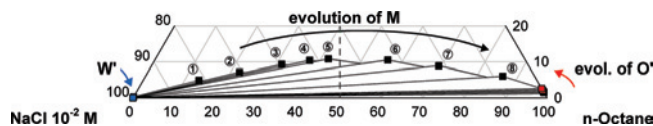
To determine these points, it is convenient to locate the coordinates of points W', O', and M in a Cartesian system with fw as the abscissa axis and the surfactant concentration as the ordinate. In this coordinates system, the W'–M, O'–M, and W'–O' segments that define the triphasic zone on  $\Delta$  can be drawn. From the intersection of each segment W'–M, O'–M, and W'–O' (at each temperature) with the vertical straight lines (at constant fw) and horizontal lines (at constant surfactant concentration), the numerical values of the coordinates of these points can be determined.

With this methodology it is possible to define the triphasic zone in  $\gamma$  at any fw and in  $\chi$  at any surfactant concentration, which provides more information on the system than determining the  $\Delta$  diagrams from the  $\gamma$  cut at various fw.<sup>34</sup> More generally, it may be said that the systematical study of any cut of the phase prism SOW–temperature allows one to plot the two others.

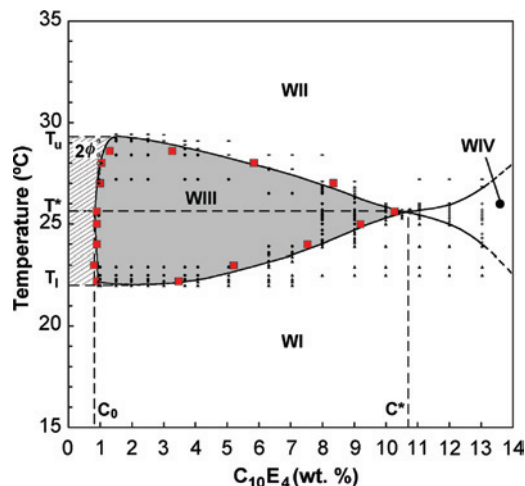
**3.1.2. Experimental Determination of the Triphasic Domain at Different Temperatures in the  $\Delta$  Cut.** The phase behavior of systems formulated with nonionic surfactants (here C<sub>10</sub>E<sub>4</sub>) is highly temperature-dependent.<sup>19</sup> The  $\Delta$  diagrams presented below correspond to the pseudoternary diagrams C<sub>10</sub>E<sub>4</sub>/n-octane/10<sup>-2</sup> M NaCl in the temperature range of 22.2–28.6 °C over which WIII systems are exhibited.

Table 1 gives the composition of the O' and M phases at 22.2, 23.0, 24.0, 25.0, 25.6, 27.0, 28.0, and 28.6 °C, as obtained by the analysis of the phases by gas chromatography. The aqueous excess phase was not analyzed in this study, and the concentrations of C<sub>10</sub>E<sub>4</sub> and n-octane in this phase were assumed to be zero. Actually, the concentration of C<sub>10</sub>E<sub>4</sub> is close to its critical micelle concentration (cmc;  $6.1 \times 10^{-4}$  M in pure water at 25 °C)<sup>43</sup> and the n-octane concentration is close to its solubility limit ( $7.5 \times 10^{-6}$  M in pure water at 25 °C).<sup>44</sup> Both figures are essentially negligible in a weight percent scale inventory.

The temperature variation of the system induces a change in the hydrophilic–lipophilic tendency of the surfactant C<sub>10</sub>E<sub>4</sub> that



**Figure 3.** Evolution of the positions of points O' and M, representative of the oil and microemulsion phases at equilibrium on  $\Delta$  for the WIII behavior of the C<sub>10</sub>E<sub>4</sub>/n-octane/10<sup>-2</sup> M NaCl system when temperature increases from 22.2 to 28.6 °C.



**Figure 4.**  $\gamma$  phase diagram of the C<sub>10</sub>E<sub>4</sub>/n-octane/10<sup>-2</sup> M NaCl system at fw = 0.5. The black symbols represent the phase behaviors experimentally determined that define the 2 $\phi$  ( $\square$ ), WI ( $\blacktriangle$ ), WII ( $-$ ), WIII ( $\bullet$ ), and WIV ( $+$ ) zones. The solid black line indicates the frontier between these zones. The red squares represent the same frontier inferred from the geometrical relation between  $\Delta$  and  $\gamma$ .

modifies considerably the composition of the microemulsion phase and the surfactant concentration in the excess oil phase,<sup>23</sup> as first evidenced a few decades ago.<sup>45</sup>

As a consequence, in the  $\Delta$  diagram, the point M which is representative of the microemulsion phase, is moved from the water side (W') to the oil side (O') when the temperature increases over only a few degrees span. Point O' representative of the oil excess phase is slightly displaced. These evolutions are represented in Figure 3 that was built from the data presented in Table 1. The shift of point M from the left to the right-hand side (positions 1–8) in the figure corresponds to an increase in temperature from 22.2 to 28.6 °C, a quite limited range, though wide enough to completely swap the affinity of C<sub>10</sub>E<sub>4</sub> from the aqueous to the oil phase.

On Figure 3, the slope of the W'–O' tie-line indicates the lipophilic tendency of the surfactant (%C<sub>10</sub>E<sub>4</sub> in O' > %C<sub>10</sub>E<sub>4</sub> in W') in the studied system, as usual for such nonionic polyethoxylated surfactant.<sup>46</sup>

**3.1.3. Confrontation of the Deduced Three-Phase Domain with the Experimental One on the  $\gamma$  and  $\chi$  Representations.**

The data presented in Table 1 were used to define the Winsor III domain on the  $\gamma$  representation at fw = 0.5 thanks to the geometrical analysis detailed in section 3.1.1. The obtained points are represented in Figure 4 by the red squares. To validate the results deduced from the GC analysis of the phases, the complete  $\gamma$  diagram at the same fw (0.5) was determined experimentally by visual observation. The resulting  $\gamma$  plot is presented in Figure 4. The black marks represent the phase behavior determined by visual observation, with a precision of  $\pm 0.1$  °C. The resulting frontier between the different behaviors (WI, WII, WIII, and WIV) is drawn as a solid black line.

The Winsor III zone (indicated in gray in Figure 4) extends between  $T_l = 22.0$  °C and  $T_u = 29.2$  °C and for C<sub>10</sub>E<sub>4</sub>

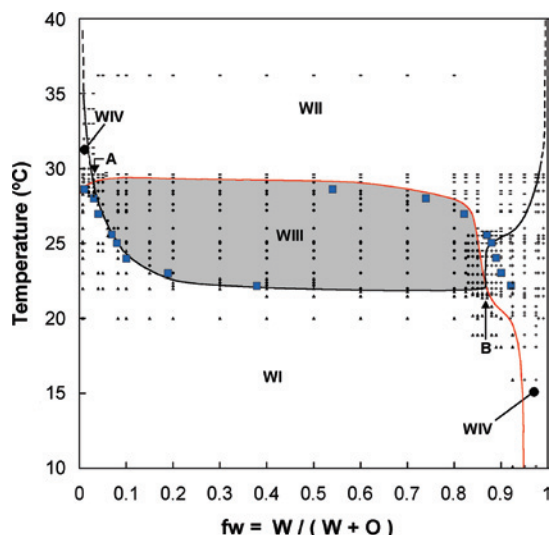


**Figure 5.**  $\chi$  phase diagram of the 3%  $C_{10}E_4/n$ -octane/ $10^{-2}$  M NaCl system. The black symbols represent the phase behaviors experimentally determined that define the WI (▲), WII (—), WIII (●), and WIV (+) zones. The solid red and black lines represent the frontiers between these domains. The blue squares represent the same frontiers inferred from the geometrical relation between  $\Delta$  and  $\chi$ .

concentrations comprised between  $C_0 = 0.9\%$  and  $C^* = 10.8\%$ . On both sides of the so-called “fish body”, WI (low temperatures) and WII (high temperatures) zones are found.

Beneath the “fish head”, a biphasic region  $2\phi$  (shaded) is found, where no microemulsion can be formed. For surfactant concentrations higher than  $C^*$  in the “fish tail”, a monophasic WIV domain is found.

On this representation, the definitions of the extent of the triphasic domain by both methods are in excellent agreement. Moreover, the described analytical method resolves some experimental limitations of the visual observation method for the determination of the WIII frontier near  $C_0$ . In this region, it is indeed difficult to formulate samples in a very limited concentration range around  $C_0$ .

In the same way, the coordinates of the points that define the triphasic domain on the  $\chi$  representation can be obtained. They are represented by the blue squares in Figure 5 for a cut at 3% surfactant. In the same figure, the complete  $\chi$  diagram obtained by visual observation is also drawn.

The red and black lines are the surfactant–oil and surfactant–water solubility curves, respectively.<sup>47</sup> The two intersection points are denoted A (high oil content) and B (high water content) and define the limits between the triphasic WIII and the monophasic WIV zones.

The Winsor III zone (in gray in Figure 5) is observed below the surfactant–oil solubility curve and above the surfactant–water solubility curve between points A and B. Between the solubility curves for fw lower than  $fw_A$  and higher than  $fw_B$ , two monophasic Winsor WIV regions extend. Aside the previously defined WIII and WIV zones, two biphasic regions are observed, i.e., of the WI type at low temperature and WII type at high temperature.

Here also, a good correlation between the frontiers defined by both methods is obtained, except for the points at fw close to 1, because of the limitation of the aqueous phase composition approximation. Experimental data with systems containing 1 and 7% surfactant (not shown here) corroborate the good correlation between both methods. All these results validate the method to determine the extent of the triphasic zone in  $\gamma$  and

$\chi$  diagrams from the analysis of a series of  $\Delta$  diagrams at different temperatures. More generally, from the systematic analysis of any cut of the phase prism, it is possible to map the phase behavior in the two other cuts.

Next, this method is applied to follow the evolution of the extent of the three-phase zone in the  $\gamma$  cut with fw changes and in the  $\chi$  cut when the surfactant concentration is altered.

**3.2. Use of the Method To Study the Variation of the Triphasic Domain in  $\gamma$  and  $\chi$  Cuts and Its Relation with the Surfactant O/W Partitioning.** In this section, the coordinates of point M of the  $\Delta$  diagrams are called  $(C_M, T_M)$  in the  $\gamma$  representation. These coordinates correspond to the point of minimum surfactant concentration at which a WIV microemulsion is obtained for a given fw. For the particular case  $fw = 0.5$ , these coordinates were previously called  $(C^*, T^*)$ .

Figure 6 shows that as the proportion of water increases, less surfactant is needed to attain a three-phase system (decrease of  $C_0$  value), since the triphasic zone of the  $\gamma$  diagram gets closer to the ordinates axis. This effect is correlated with the slanting of the W'–O' line in the  $\Delta$  diagram shown in Figure 3. The same effects have been observed in the case of hydrotropes such as  $C_4E_1$ , which is also quite lipophilic.<sup>34</sup>

Table 2 shows the concentration and temperature values corresponding to the characteristic points of the  $\gamma$  phase diagram, for fw values between 0.1 and 0.9. These values are in good agreement with the ones reported previously<sup>34</sup> (10.7% at  $fw = 0.5$  and for a salt-free water phase). It should be noted that since fw is expressed in weight fraction, the formulation corresponding to equal volumes of oil and water corresponds in this case to  $fw \sim 0.6$ . For this value,  $C_M$  is found equal to 10.1%, which is also in fairly good agreement with what is reported in the literature (9.9% in the case of a pure water phase<sup>16</sup>).

For equal volumes of oil and water, the triphasic zone shape in the  $\gamma$  cut ( $fw \sim 0.6$  in Figure 6) is symmetrical with respect to the horizontal axis at  $T_M$ . For high fw, the triphasic zone extends more toward lower temperatures, which means that an increase in the proportion of the aqueous phase tends to favor its solubilization in the microemulsion. Similarly, for low fw, the solubilization of the oil phase in the microemulsion becomes more important. These results are in agreement with the upward or downward slanting of the three-phase region in the  $\gamma$  cut observed in the case of short-chain  $C_iE_j$ .<sup>33,34</sup>

The method also enlightens the fact that, for fw higher than 0.5, the coordinates of the limit point  $(C_M, T_M)$  decrease when fw increases. For fw lower than 0.5,  $C_M$  increases and  $T_M$  decreases when fw increases. Actually, the evolution of  $C_M$  as a function of fw exhibits a parabolic shape,<sup>48</sup> as already described for short-chain  $C_iE_j$ .<sup>33</sup> For the studied system, the maximum is obtained for  $fw \sim 0.45$ ,<sup>48</sup> which corresponds neither to equal masses nor to equal volumes of oil and water. If  $C_M$  is related to the surfactant efficiency as proposed by Kahlweit for equal amounts of oil and water, these data evidence that the efficiency of a surfactant depends on the water–oil ratio.<sup>29</sup> These results are of major interest as far as applications are concerned, since they give the minimum surfactant concentration required to attain a monophasic WIV system for a given fw.

The evolution of the extent of the triphasic zone in the  $\chi$  diagram could be determined in the same way as a function of the surfactant concentration. Figure 7 shows the evolution of the three-phase domain on  $\chi$  cut at various surfactant concentrations.

This figure shows that when the  $C_{10}E_4$  concentration increases from 0.5 to 2.5%, the triphasic zone progressively extends to the left, i.e., in the direction of low fw. In this concentration range the  $\chi$  representations exhibit an unusual shape in which

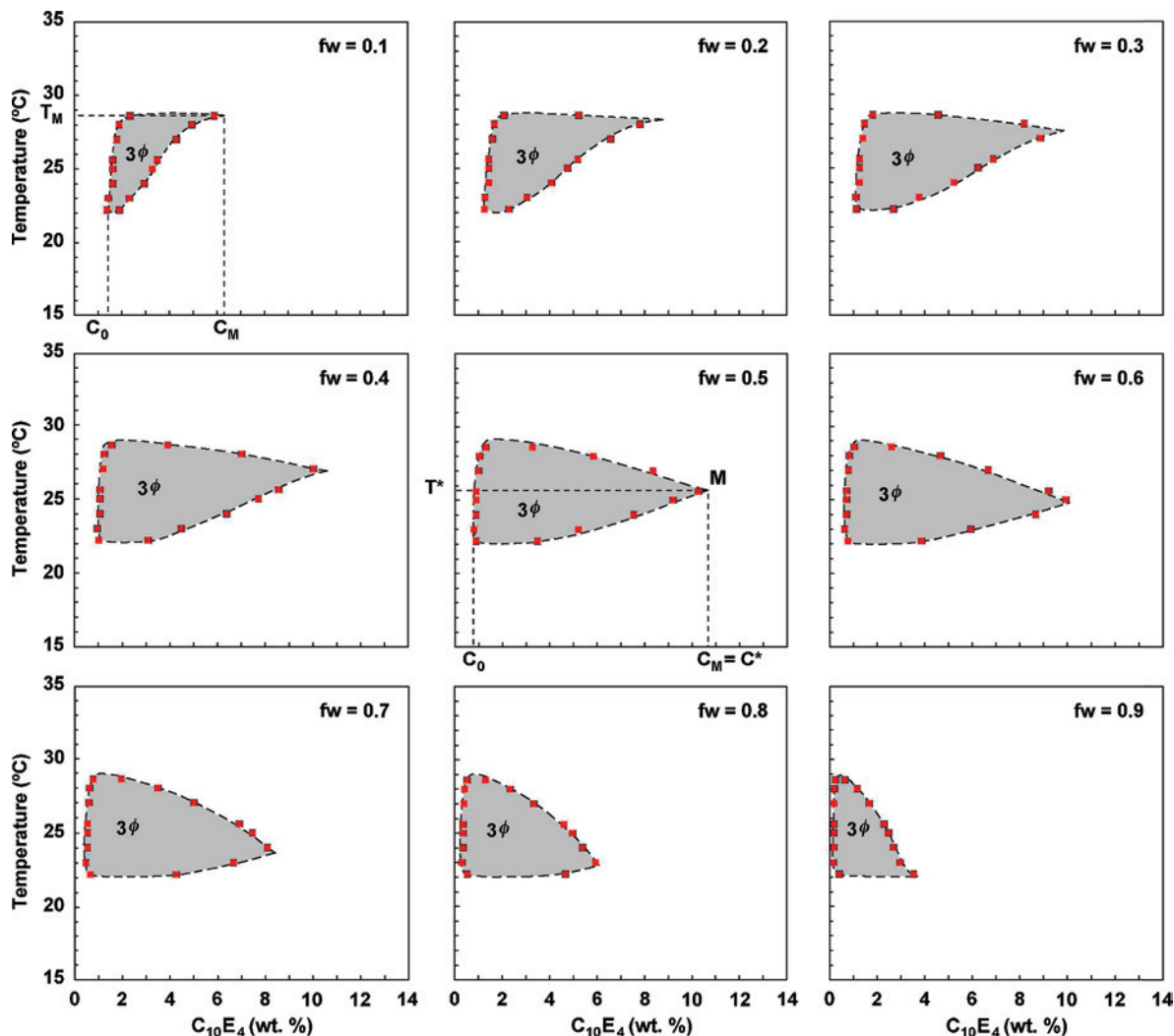


**Figure 6.** Evolution of the triphasic zone shape in the  $\gamma$  cut as a function of  $fw$ , inferred from the geometrical relation between  $\Delta$  and  $\gamma$  cuts. The red squares are obtained from the experimental points shown in Figure 3. The dashed lines represent the estimated boundaries of the WIII domains.

**TABLE 2: Surfactant Concentrations  $C_0$  and  $C_M$  and Temperatures  $T_M$  for  $\gamma$  Phase Diagrams at Different  $fw$  Extrapolated from Figure 6**

$fw$	$C_0$ (% $C_{10}E_4$ )	$C_M$ (% $C_{10}E_4$ )	$T_M$ (°C)
0.1	1.4	6.2	28.5
0.2	1.3	8.8	28.2
0.3	1.1	9.8	27.5
0.4	1.0	10.6	26.8
0.5	0.9	10.8	25.7
0.6	0.6	10.1	24.8
0.7	0.5	8.4	23.6
0.8	0.3	6.0	22.7
0.9	0.2	3.6	22.1

junction point A (see Figure 5) has disappeared. For concentration higher than 2.5%, the WIII zone progressively shrinks as the surfactant concentration increases. In this range, the usual three-phase body is exhibited with both extreme A and B junction points.

The expansion of the area of the WIII region with the surfactant concentration in the low concentration range has not been previously reported in the literature which only describes the behavior obtained at higher concentrations, i.e., the progressive disappearance of the WIII body.<sup>11,17,18,20,29,35,45,49</sup>

This unusual behavior may be explained by carefully looking at the correspondence between the  $\Delta$  and  $\chi$  phase diagrams.

Figure 8 shows schematically the relation between these two diagrams for the  $C_{10}E_4/n$ -octane/water system. Parts a, b, and d of Figure 8 illustrate the three possible aspects of the  $\chi$  cut at high (12%), medium (3%), and low (1%) surfactant concentrations, respectively. In Figure 8c the  $\Delta$  diagram at  $T = T^*$  is represented and vertically amplified; i.e., the S apex corresponding to 100% surfactant has been shifted to infinity so that vertical lines follow a constant  $fw$  value, as in other plots.

The main characteristic feature of the  $\Delta$  diagram of this system is the slanting of the bottom tie line  $O'-W'$  of the triangle that limits the WIII region from below. This inclination is due to the unequal partitioning of the surfactant between the oil and water phases, which is accountable for the existence of the unusual new shape encountered at low surfactant concentration (Figure 8d).

If a horizontal line is drawn on Figure 8  $\Delta$  diagram at 3% surfactant, WIV, WI, WIII, WII, and WIV zones are successively crossed when moving from the oil side to the water side, i.e., when increasing  $fw$ . The correspondence with the  $\chi$  representation at 3% surfactant indicates the same succession for  $T = T^*$  (Figure 8b). The biphasic regions (WI and WII) in the  $\chi$  cut correspond to the biphasic lobes in the  $\Delta$  cut. For this surfactant concentration, the two junction points A and B between the WIII and WIV zones at low and high  $fw$  are present.

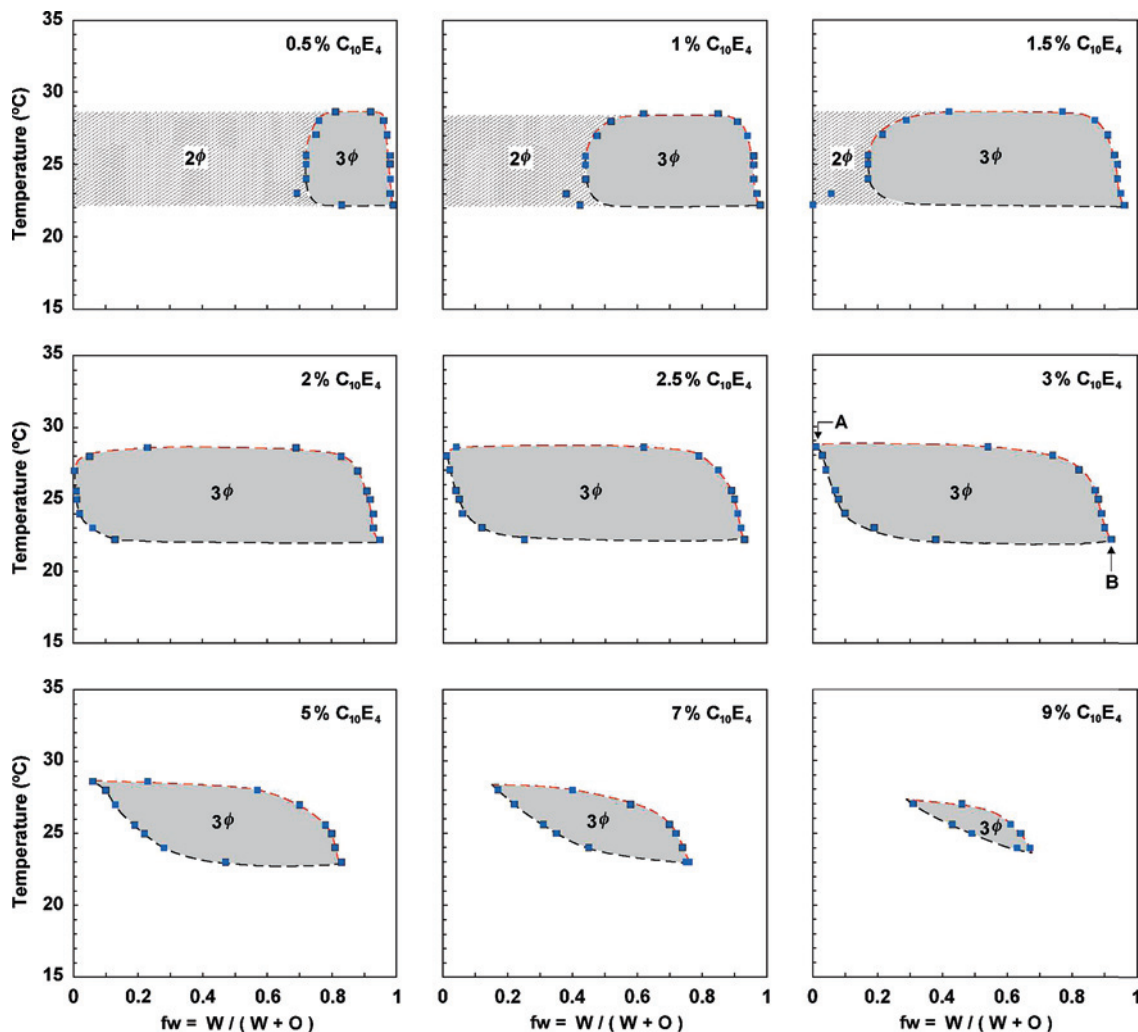


**Figure 7.** Evolution of the extent of the triphasic zone in the  $\chi$  cut as a function of the surfactant concentration, inferred from the geometrical relation between  $\Delta$  and  $\chi$  cuts. The blue squares are obtained from the experimental points shown in Figure 3. The dashed red and black lines represent the estimated boundaries of the WIII domain.

These two points are not situated at the same temperature because of the existence of the two biphasic lobes. This kind of behavior is encountered for a surfactant concentration in the  $C_O$  to  $C_M$  range.

For surfactant concentration higher than  $C_M$  (for example 12%), a horizontal line crosses successively the WIV, WI, WIV, WII, and WIV zones, which gives rise to the type of  $\chi$  cut represented schematically in Figure 8a. This kind of behavior is observed for concentration between  $C_M$  and the highest concentration for which a horizontal line still crosses both biphasic lobes in  $\Delta$ . It may be noted that the two junction points A and B have disappeared and that the polyphasic zones are separated. At higher concentration, these two polyphasic zones are farther away and a horizontal line at  $T = T^*$  only crosses the WIV zone.

At low surfactant concentration, for instance 1%, a horizontal line crosses successively the WIV,  $2\phi$ , WIII, WII, and WIV regions in the  $\Delta$  cut. On the  $\chi$  representation the  $2\phi$ -zone situated on the left-hand side corresponds to the zone below the  $W'-O'$  bottom tie line, where the surfactant concentration is too low to produce a microemulsion. This type of unusual shape in a  $\chi$  cut is found at concentration below  $C_O$  and evidences the unequal partitioning of the surfactant in favor of the oil phase.

This unequal partitioning can be corroborated by calculating the value of the standard free energy of transfer  $\Delta G^\circ$  of the

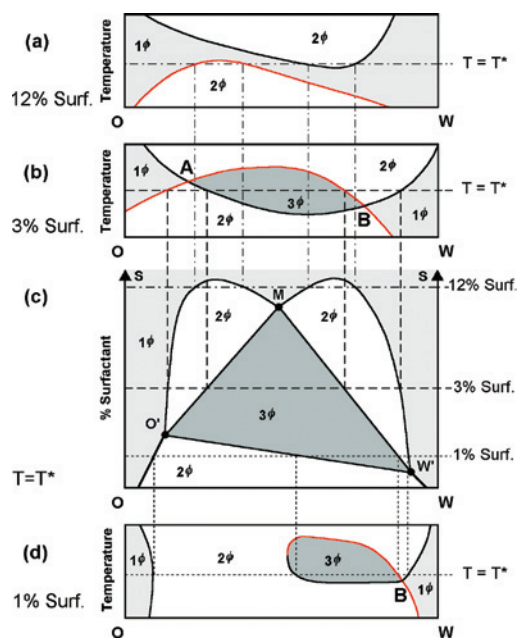


**Figure 8.** Schematic representation of the  $\Delta$  and  $\chi$  diagrams for a SOW system as  $C_{10}E_4/n$ -octane/ $10^{-2}$  M NaCl. The  $\chi$  diagrams are plotted at three surfactant concentrations 12 (a), 3 (b), and 1% (d) indicated by horizontal lines in the  $\Delta$  diagram (c).

surfactant from the water phase to the oil phase. The partition coefficient can easily be obtained from the measurement of the surfactant concentrations in the excess oil and aqueous phases. It should be noted that the partition coefficient has to be measured in diluted solutions to warrant that the surfactant is in a monomeric state. In Winsor III systems, the presence of the microemulsion middle phase guarantees that the excess phases are micelle-free and thus complies with this requirement.<sup>50</sup>

The chemical potentials of  $C_{10}E_4$  in the excess oil and water phases  $\mu_{O'}$  and  $\mu_{W'}$ , respectively, may be written as follows:

$$\mu_{W'} = \mu_{W'}^{\circ} + RT \ln a_{W'} \quad (1)$$

$$\mu_{O'} = \mu_{O'}^{\circ} + RT \ln a_{O'} \quad (2)$$

where  $\mu_{W'}^{\circ}$  and  $\mu_{O'}^{\circ}$  are the standard chemicals potentials and  $a_{W'}$  and  $a_{O'}$  are the activities of  $C_{10}E_4$  in the excess water and oil phases ( $W'$  and  $O'$ ). Because of the low concentrations in both excess phases, the activity coefficients are often supposed to be unity and the activities are thus estimated by the concentrations, which may not be a good approximation in all cases. At equilibrium,  $\mu_{W'} = \mu_{O'}$ , which leads to

$$\Delta G^{\circ} = \mu_{O'}^{\circ} - \mu_{W'}^{\circ} = -RT \ln \frac{C_{O'}}{C_{W'}} = -RT \ln K_{O'W'} \quad (3)$$

At  $T = 25^{\circ}\text{C}$ ,  $C_{O'} = 1.8 \text{ wt } \%$  (cf. Table 1) and  $C_{W'} \approx \text{cmc}$  in water at  $25^{\circ}\text{C}$  (0.017%),<sup>43</sup> and consequently the partition coefficient  $K_{O'W'}$  is close to 100, and  $\Delta G^{\circ} \approx -11.6 \text{ kJ/mol}$ , which confirms a partitioning of  $C_{10}E_4$  strongly in favor of the oil phase. When  $T$  increases,  $C_{O'}$  increases and  $C_{W'}$  decreases as is usually observed for polyethoxylated nonionic surfactants. These results are in agreement with what is generally obtained for such systems.<sup>46</sup>

It is worth remembering here that the strongly biased partitioning between oil and water at optimum formulation has been mostly associated to polydistributed nonionic surfactant mixtures of oligomers. For such commercial systems, the partitioning of the different oligomers results in an interfacial mixture which depends on the total surfactant concentration and water-to-oil ratio.<sup>51,52</sup> As a consequence the actual optimum formulation, which is here determined by the temperature at the middle of the three-phase behavior region, depends on both surfactant concentration and water-to-oil ratio. The following figure exhibits a slight slope for this three-phase behavior centerline when the water-to-oil ratio varies. Hence, it clearly indicates that this interfacial formulation shift also occur with isomerically pure surfactants, although maybe not to the extent it has been reported for widely distributed mixture. It may be thus concluded that it is due, not to a selective partitioning or fractionation, but to the unequal partitioning between oil and water.<sup>46,53,54</sup> This corroborates the fact that anionic surfactants, even very polydispersed ones, exhibit a partitioning coefficient close to unity,<sup>55</sup> whereas polyethoxylated nonionics are found in a much higher concentration in the oil phase at equilibrium, even when they are significantly hydrophilic, whatever they are commercial mixtures or isomerically pure substances.

The unusual shape predicted at low surfactant concentration has been confirmed by the experimental determination of the  $\chi$  diagram at 1%  $C_{10}E_4$  presented in Figure 9. In this diagram

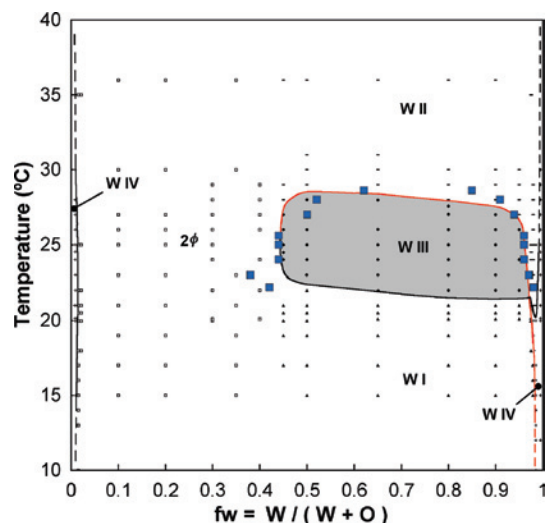


**Figure 9.**  $\chi$  phase diagram of the 1% $C_{10}E_4/n$ -octane/ $10^{-2}$  M NaCl system. The black symbols represent the phase behaviors experimentally determined that define the  $2\phi$  ( $\square$ ), WI ( $\blacktriangle$ ), WII ( $\text{---}$ ), WIII ( $\bullet$ ), and WIV ( $+$ ) zones. The solid red and black lines represent the frontiers between these domains. The blue squares represent the same frontier inferred from the geometrical relation between  $\Delta$  and  $\chi$ .

junction point A (see Figure 5) has vanished, and on the left-hand side there is a  $2\phi$ -zone where no microemulsion can be formed in the 0–0.44 fw range.

#### 4. Conclusions

A systematic study of the phase behavior of a well-defined SOW–T system based on a pure oil ( $n$ -octane) and an oligomerically pure surfactant ( $C_{10}E_4$ ) allowed to revisit the correlation between the three usual cuts of the phase prism, namely, the  $\gamma$  (constant water–oil ratio),  $\chi$  (constant surfactant concentration), and  $\Delta$  (constant temperature) representations. The systematic analysis of any cut of the phase prism allows one to generate the two others in a straightforward manner. In our case, the  $\gamma$  and  $\chi$  cuts were obtained from the study of  $\Delta$  diagrams at different temperatures. More generally, this methodology may be applied to any SOW ternary system and any formulation variable, i.e., a variable that modifies the affinity of the surfactant for the aqueous and oil phases, such as salinity, the nature of the oil (ACN), and pH, etc.

This study showed for the first time the evolution of the WIII zone shapes in  $\gamma$  and  $\chi$  cuts with fw and with the surfactant concentration, for a true ternary system. The evolution of the phase behavior in the  $\gamma$  cut evidences that the efficiency of a surfactant depends on the water–oil ratio, an issue that is of major relevance as far as applications are concerned. The results provide the minimum surfactant concentration needed to attain a monophasic WIV system for a given fw. The WIII zone in the  $\chi$  cut exhibits an unusual shape at low surfactant concentration (lower than  $C_{O'}$ ) that is a direct consequence of the unequal partitioning of the surfactant between the aqueous and oil phases. In this low concentration range, the extent of the triphasic domain increases with the surfactant concentration. For concentration between  $C_{O'}$  and  $C_M$ , the usual shrinking of the WIII domain is observed as the surfactant concentration increases.

**Acknowledgment.** The University of The Andes Scholarship Program is thanked for providing financial help to carry out this project. University Lille 1, Polytech-Lille is gratefully acknowledged for a grant to A.P. as an invited professor.

## References and Notes

- (1) Shinoda, K.; Saito, H. *J. Colloid Interface Sci.* **1968**, *26*, 70–74.
- (2) Salager, J. L.; Loaiza, I.; Miñana, M.; Silva, F. *J. Dispersion Sci. Technol.* **1982**, *3*, 279–292.
- (3) Kabalnov, A.; Weers, J. *Langmuir* **1996**, *12*, 1931–1935.
- (4) Salager, J. L.; Forgiarini, A.; Marquez, L.; Peña, A.; Pizzino, A.; Rodriguez, M. P.; Rondün, M. *Adv. Colloid Interface Sci.* **2004**, *108*, 259–272.
- (5) Salager, J. L. *Emulsion Phase Inversion Phenomena*. In *Emulsions and Emulsion Stability*, 2nd ed.; Sjöblom, J., Ed.; Taylor and Francis: London, 2006; pp 185–226.
- (6) Salager, J. L.; Morgan, J. C.; Schechter, R. S.; Wade, W. H.; Vasquez, E. *Soc. Pet. Eng. J.* **1979**, *19*, 107–115.
- (7) Kunieda, H.; Friberg, S. E. *Bull. Chem. Soc. Jpn.* **1981**, *54*, 1010–1014.
- (8) Kunieda, H.; Shinoda, K. *Bull. Chem. Soc. Jpn.* **1982**, *55*, 1777–1781.
- (9) Winsor, P. A. *Chem. Rev.* **1968**, *68*, 1–40.
- (10) Salager, J. L.; Anton, R.; Aubry, J. M. *Tech. Ing.* **2006**, *41* (J 124), J2158/1–J2158/17.
- (11) Kahlweit, M.; Lessner, E.; Strey, R. *J. Phys. Chem.* **1983**, *87*, 5032–5040.
- (12) Salager, J. L.; Miñana, M.; Perez, M.; Ramirez, M.; Rojas, C. I. *J. Dispersion Sci. Technol.* **1983**, *4*, 313–329.
- (13) Bourrel, M.; Salager, J. L.; Lipow, A. M.; Wade, W. H.; Schechter, R. S. *Properties of Amphiphile-Oil-Water Systems at Optimum Formulation for Phase Behavior*, 53rd Annual Fall Technical Conference, Oct. 1–3, 1978; Society of Petroleum Engineers: Houston, TX, 1978; paper SPE 7450.
- (14) Sottmann, T.; Strey, R. *J. Chem. Phys.* **1997**, *106*, 8606–8615.
- (15) Kahlweit, M.; Strey, R.; Haase, D.; Kunieda, H.; Schmeling, T.; Faulhaber, B.; Borkovec, M.; Eicke, H. F.; Busse, G.; Eggers, F.; Funck, Th.; Richmann, H.; Magid, L.; Södermann, O.; Stilbs, P.; Winkler, J.; Dittrich, A.; Jahn, W. *J. Colloid Interface Sci.* **1987**, *118*, 436–453.
- (16) Sottmann, Th.; Stubenrauch, C. Phase Behaviour, Interfacial Tension and Microstructure of Microemulsions. In *Microemulsions*; Stubenrauch, C., Ed.; Wiley: Chichester, U.K., 2009; pp 1–47.
- (17) Sjöblom, J.; Lindberg, R.; Friberg, S. E. *Adv. Colloid Interface Sci.* **1996**, *65*, 125–287.
- (18) Shinoda, K. Solvent Properties of Non-ionic Surfactants in Aqueous Solutions. In *Solvent Properties of Surfactant Solution*; Shinoda, K., Ed.; Dekker: New York, 1967; pp 27–63.
- (19) Kunieda, H.; Shinoda, K. *J. Dispersion Sci. Technol.* **1982**, *3*, 233–244.
- (20) Shinoda, K.; Kunieda, H.; Arai, T.; Saijo, H. *J. Phys. Chem.* **1984**, *88*, 5126–5129.
- (21) Lichtenfeld, F.; Schmeling, T.; Strey, R. *J. Phys. Chem.* **1986**, *90*, 5762–5766.
- (22) Shinoda, K.; Lindman, B. *Langmuir* **1987**, *3*, 135–149.
- (23) Kahlweit, M.; Strey, R.; Busse, G. *Phys. Rev. E* **1993**, *47*, 4197–4209.
- (24) Aratono, M.; Kahlweit, M. *J. Chem. Phys.* **1991**, *95*, 8578–8583.
- (25) Sottman, T.; Strey, R. *J. Phys.: Condens. Matter* **1996**, *8*, A39–A48.
- (26) Kahlweit, M.; Strey, R. *Angew. Chem., Int. Ed. Engl.* **1985**, *24*, 654–668.
- (27) Kahlweit, M.; Strey, R.; Haase, D. *J. Phys. Chem.* **1985**, *89*, 163–171.
- (28) Kahlweit, M.; Strey, R.; Firman, P.; Haase, D. *Langmuir* **1985**, *1*, 281–288.
- (29) Kahlweit, M.; Strey, R.; Firman, P. *J. Phys. Chem.* **1986**, *90*, 671–677.
- (30) Kahlweit, M.; Strey, R.; Firman, P.; Haase, D.; Jen, J.; Schömäcker, R. *Langmuir* **1988**, *4*, 499–511.
- (31) Kahlweit, M.; Strey, R.; Haase, D.; Firman, P. *Langmuir* **1988**, *4*, 785–790.
- (32) Kilpatrick, P. K.; Gorman, C. A.; Davis, H. T.; Scriven, L. E.; Miller, W. G. *J. Phys. Chem.* **1986**, *90*, 5292–5299.
- (33) Rudolph, E. S. J.; Caçao, M. A.; de Loos, Th. W.; de Swaan, J. J. *Phys. Chem. B* **1997**, *101*, 3914Z–3918.
- (34) Burauer, S.; Sachert, T.; Sottmann, T.; Strey, R. *Phys. Chem. Chem. Phys.* **1999**, *1*, 4299–4306.
- (35) Kahlweit, M.; Busse, G.; Winkler, J. *J. Chem. Phys.* **1993**, *99*, 5605–5614.
- (36) Lang, J. C. *Proc. Int. Sch. Phys. "Enrico Fermi"* **1984**, *90*, 336–375.
- (37) Laughlin, R. The Influence of Third Components on Aqueous Surfactant Phase Behavior. In *The Aqueous Phase Behavior of Surfactants*; Ottewill, R. H.; Rowell, R. L., Eds.; Academic Press: New York, 1994; pp 368–416.
- (38) Gibson, T. *J. Org. Chem.* **1980**, *45*, 1095–1098.
- (39) Lang, J. C.; Morgan, R. D. *J. Chem. Phys.* **1980**, *73*, 5849–5861.
- (40) Queste, S.; Salager, J. L.; Strey, R.; Aubry, J. M. *J. Colloid Interface Sci.* **2007**, *312*, 98–107.
- (41) Schlarmann, J.; Stubenrauch, C.; Strey, R. *Phys. Chem. Chem. Phys.* **2003**, *5*, 184–191.
- (42) Winsor, P. *Solvent Properties of Amphiphilic Compounds*; Butterworth: London, 1954.
- (43) Eastoe, J.; Dalton, J. S.; Rogueda, Ph. G. A.; Crooks, E. R.; Pitt, A. R.; Simister, E. A. *J. Colloid Interface Sci.* **1997**, *188*, 423–430.
- (44) Sarraute, S.; Delepine, H.; Costa, M. F.; Majer, V. *Chemosphere* **2004**, *57*, 1543–1551.
- (45) Shinoda, K.; Kunieda, H. Phase Properties of Emulsions: PIT and HLB. In *Encyclopedia of Emulsion Technology*, Vol. 1, Basic Theory; Becher, P., Ed.; Dekker: New York, 1983; pp 337–367.
- (46) Ben Ghoulam, M.; Moatadid, N.; Graciaa, A.; Lachaise, J. *Langmuir* **2002**, *18*, 4367–4371.
- (47) Shinoda, K. *Progr. Colloids Polym. Sci.* **1983**, *68*, 1–7.
- (48) Pizzino, A. *Inversion de Phase des Emulsions: Relation avec le Comportement à l'Equilibre et Détection par Rétroréflexion de Lumière*. Ph.D. Thesis, Université des Sciences et Technologies de Lille, September 2008.
- (49) Kunieda, H.; Yamagata, M. *Colloid Polym. Sci.* **1993**, *271*, 997–1004.
- (50) Salager, J. L.; Marquez, N.; Graciaa, A.; Lachaise, J. *Langmuir* **2000**, *16*, 5534–5539.
- (51) Graciaa, A.; Lachaise, J.; Sayous, J. G.; Grenier, P.; Yiv, S.; Schechter, R. S.; Wade, W. H. *J. Colloid Interface Sci.* **1983**, *93*, 474–486.
- (52) Buzier, M.; Ravey, J. C. *J. Colloid Interface Sci.* **1983**, *91*, 20–33.
- (53) Graciaa, A.; Andérez, J.; Bracho, C.; Lachaise, J.; Salager, J. L.; Tolosa, L.; Ysamertt, F. *Adv. Colloid Interface Sci.* **2006**, *123*, 63–73.
- (54) Ben Ghoulam, M.; Moatadid, N.; Graciaa, A.; Lachaise, J. *Langmuir* **2004**, *20*, 2584–2589.
- (55) Wade, W. H.; Morgan, J. C.; Schechter, R. S.; Jacobson, J. K.; Salager, J. L. *Soc. Pet. Eng. J.* **1978**, *18*, 242–252.